Construction and Building Materials 24 (2010) 2542–2553

Contents lists available at ScienceDirect

Construction and Building Materials

journal homepage: www.elsevier.com/locate/conbuildmat

# Nonlinear concrete model for double-skinned composite tubular columns

Taek Hee Han [a], J. Michael Stallings [b], Young Jong Kang [c,*]

[a] R&D Center, Seoul Metro, Seoul 156-080, Republic of Korea
[b] Department of Civil Engineering, Auburn University, Auburn, AL 36830, USA
[c] Department of Architectural, Civil and Environmental Engineering, Korea University, Seoul 156-701, Republic of Korea

ARTICLE INFO

*Article history:*
Received 18 June 2008
Received in revised form 3 March 2010
Accepted 1 June 2010
Available online 30 June 2010

*Keywords:*
Column
Concrete
Nonlinear
DSCT
Confinement

ABSTRACT

The use of concrete filled steel tube (CFT) columns is growing because of their superior performance. However, in some applications, CFT columns might be uneconomical or massive because they should be fully filled with concrete. To overcome these disadvantages, double-skinned composite tubular (DSCT) columns were suggested and have been studied by many researchers. In this study, a nonlinear concrete model was suggested for the analysis of DSCT columns. The model was developed by modifying Mander et al.'s unified concrete model. The stress–strain model of the concrete in a DSCT column was defined by identifying the possible failure modes of the column and deriving the equations for the confining pressure for each failure mode from equilibriums. By using derived equations, a computer program was coded and parametric studies were performed for some examples. The analysis results were verified by comparisons with the experimental results from other researchers. The proposed nonlinear concrete model explains why a DSCT column has enhanced strength beyond the sum of the strengths of its component parts which are an inner tube, an outer tube, and unconfined concrete.



## 1. Introduction

Columns and footings are the main members resisting axial force and lateral seismic force. Therefore, the behavior of a column has a significant effect on the whole structure. And an analytical model simulating the column behavior is required to define the behavior of a structure. However, concrete filled steel tube (CFT) columns are not popular for bridge piers whereas reinforced concrete (RC) columns are widely used. This results from the large diameter of a typical bridge pier. If a CFT column can have a reduced cross section or reduced self-weight without the loss of its capacity, it will be convenient to use a CFT column as a bridge pier. When a column is designed, the confining effect of concrete is not considered in many cases although there is a significant difference between the behaviors of confined concrete and unconfined concrete. Therefore, it is necessary to consider the confining effect and nonlinearity of concrete for the accurate and economic design of a column. Although a hollow RC column has been widely used to reduce their material and self-weight, its ductility and strength cannot be guaranteed because its concrete is under not triaxial but biaxial confinement. This biaxially confined state might be the cause of brittle failure or low-strength of the column. To overcome these problems, an internally confined hollow (ICH) RC member, which is a hollow RC member with an internal steel tube to make its concrete be under triaxial confinement, was presented in 2008 [1].

To save the material cost and enhance the performance of a CFT column, a double-skinned composite tubular (DSCT) column was developed in late 1980s [2]. Fig. 1 shows a typical cross section of a DSCT column. Double steel tubes are arranged and concrete is filled between them. After the introduction of a DSCT column by Shakir-Khalil and Illouli [2], it has been studied by many researchers. Wei et al. [3,4] showed that the strength of a DSCT member is 10–30% larger than the sum of the strength of each component: concrete, the inner tube, and the outer tube. And they suggested an empirical formula for the strength of a DSCT member. Zhao and Grzebieta [5] studied the strength and ductility of a DSCT column with a square cross section in 2002. Tao et al. [6] investigated the strength and ductility of a DSCT column with a circular section in 2002. Han et al. [7] studied the energy dissipating capacity of a DSCT column and suggested a DSCT column with a corrugated steel tube as the internal tube in 2005. Recently, a double-skinned hybrid tubular (DSHT) column has been researched, which is composed of a fiber-reinforced-polymer (FRP) tube and a steel tube. Teng et al. [8] suggested its concept and behavior. Yu et al. [9] tested its flexural behavior in 2006. From many researches, most researchers agreed with the strength of a DSCT or DSHT member had larger strength than the sum of the strength of each component. However, its failure mode and the confining effect of concrete were not considered in their researches.

* Corresponding author. Tel.: +82 2 3290 3317; fax: +82 2 921 5166.
*E-mail address:* yjkang@korea.ac.kr (Y.J. Kang).

0950-0618/$ - see front matter © 2010 Elsevier Ltd. All rights reserved.
doi:10.1016/j.conbuildmat.2010.06.001

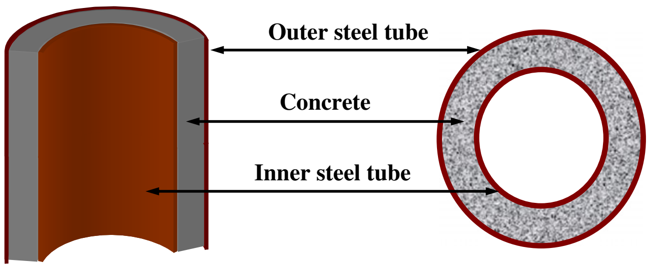


**Fig. 1.** Cross section of a circular DSCT.

The main subject of the present study is how to give triaxial confinement to the concrete in a DSCT column although it has a hollow section. In a DSCT column, the internal tube makes it possible by confining the concrete. Fig. 2 shows the triaxially confined concrete in a DSCT column. Where, $d$ is the diameter of confined concrete, $t$ is the thickness of the concrete wall, $f_1$ is axial pressure, $f_2$ is circumferential pressure, $f_3$ is radial pressure, and $f_y$ is yield stress of the outer tube. As shown in Figs. 1 and 2a, concrete is filled between the inner tube and outer tube. When the concrete is under axial load ($f_1$), the concrete inclines to enlarge its volume in lateral directions. Because the concrete is restrained by the inner and outer tubes, it cannot freely increase its volume and it is confined. Therefore, the both tubes give lateral passive pressure ($f_3$) to the concrete in the radial direction. Circumferential pressure ($f_2$) is given by the arching action of the concrete wall as shown in Fig. 2b and c. If there is no inner tube, the concrete wall will be biaxially confined as shown in Fig. 3. Considering the concrete and the outer tube are not bonded, the concrete wall can be regarded unconfined in this case. Therefore, for the accurate analysis of a DSCT column, it is necessary to define a nonlinear concrete model for the DSCT column with consideration of the confining effect.

The topic about the confining effect of concrete in a RC column has been studied by many researchers such as Roy and Sozen [10], Popovics [11], Kent and Park [12], Leslie [13], and Desayi et al. [14]. In 1988, Mander et al. [15] proposed a unified concrete model to predict the behavior of concrete under compression before and after the yield of concrete. Recently, much research about concrete confined by a tube has been performed. Candappa et al. [16] studied the behavior of a CFT column with a high-strength steel tube. The behavior of concrete confined by FRP has also been studied.

In this study, the failure mode of a DSCT column was defined and a nonlinear concrete model for a DSCT column was developed with the consideration of confining effects. Equilibrium equations were derived for each failure mode and an analysis tool was developed with FORTRAN language. The developed nonlinear concrete model is based on Mander et al. [15] unified concrete model and lateral pressures were redefined for DSCT columns.

## 2. Development of analysis model

For the moment–curvature analysis of the column under combined axial and flexural loads, it is necessary to use constitutive models which can trace the stress–strain path of the applied material. In this research, a stress–stain model of the concrete in a DSCT column is developed. Later this work will be extended to moment–curvature analyses of DSCT columns. The study reported here was performed on the base of following basic assumptions: (1) the inner tube offers complete confining pressure unless it fails; (2) the inner tube offers no confining pressure if it fails; (3) the DSCT member fails when the outer tube fails, and (4) the concrete and the tubes are not composite. The fourth assumption means the concrete is under the unconfined state if any tube fails.

### 2.1. Uniaxial stress–strain model

Mander et al. [15] proposed a unified stress–strain approach to predict the pre-yield and post-yield behavior of confined concrete members subjected to axial compressive stress. In this approach, Mander et al. [15] proposed concrete models for a monotonic compressive and tensile loading condition, a cyclic compressive and tensile loading condition, and cyclic reloading branches. One of these models is briefly reviewed to explain a new concrete model for a DSCT column.

Fig. 4 shows the form of stress–strain relation in monotonic compression for confined and unconfined concrete. Mander et al. utilized Eq. (1) proposed by Popovics [11] to develop the unified stress–strain relation of the confined concrete subjected to the monotonic compression.

$$f_c = \frac{f'_{cc} x \cdot r}{r - 1 + x^r} \qquad (1)$$

where $x = \frac{\varepsilon}{\varepsilon_{cc}}$, $r = \frac{E_c}{(E_c - E_{\sec})}$, $E_{\sec} = \frac{f'_{cc}}{\varepsilon_{cc}}$, $f_c$ = concrete stress, $f'_{cc}$ = confined strength of concrete, $\varepsilon$ = uniaxial strain, $\varepsilon_{cc}$ = strain at peak concrete strength, and $E_c$ = tangent modulus of unconfined concrete.

The tangent modulus of unconfined concrete ($E_c$) can be estimated as $5000\sqrt{f'_{cc}}$ (MPa) [15]. The peak strength of confined concrete ($f'_{cc}$) is calculated with Eq. (2). The strain at peak strength of confined concrete ($\varepsilon_{cc}$) is given as a function of the strain at peak strength of unconfined concrete ($\varepsilon_{co}$) as Eq. (3). The value of $\varepsilon_{co}$ is usually regarded as 0.002.

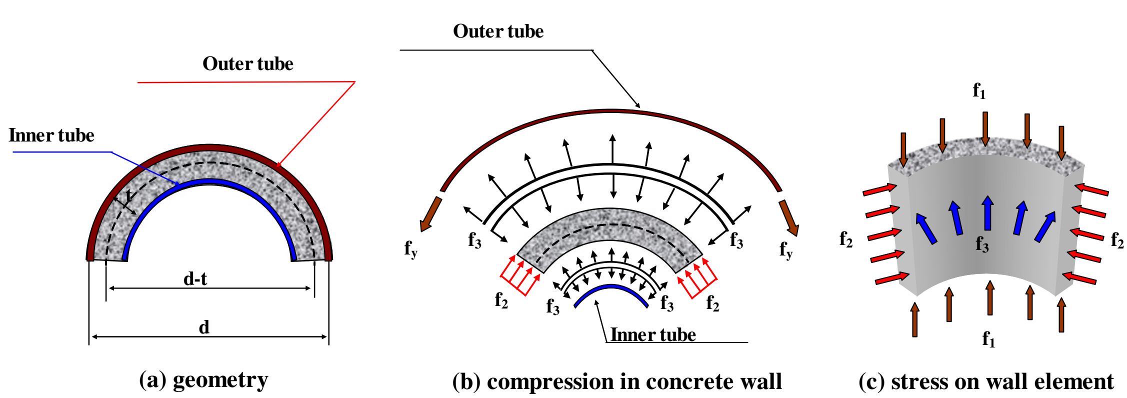


**Fig. 2.** Triaxially confined concrete in a DSCT column.

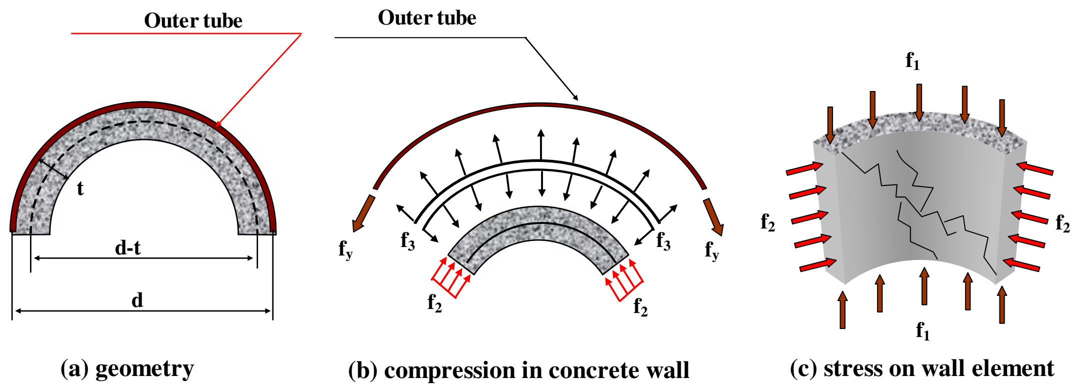


Fig. 3. Biaxially confined concrete.

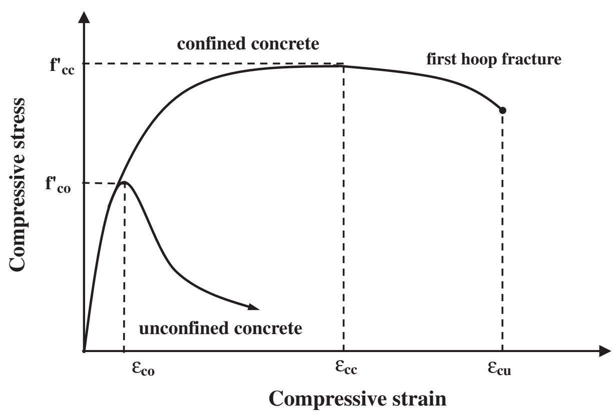


Fig. 4. Stress–strain relations of confined and unconfined concrete.

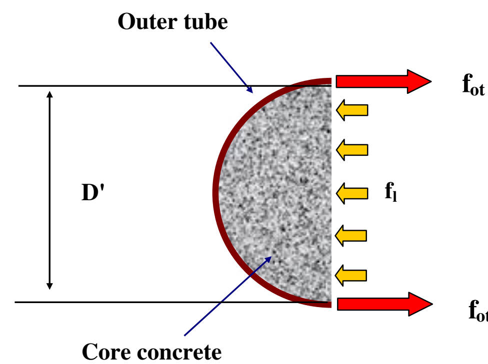


Fig. 5. Confining stress on concrete in a CFT column.

$$f'_{cc} = f'_c\left(2.254\sqrt{1+\frac{7.94f'_l}{f'_c}} - \frac{2f'_l}{f'_c} - 1.254\right) \quad (2)$$

$$\varepsilon_{cc} = \varepsilon_{co}\left[1+5\left(\frac{f'_{cc}}{f'_c}-1\right)\right] \quad (3)$$

where $f'_c$ = peak strength of unconfined concrete, $f'_l$ = effective constant lateral confining pressure, and $\varepsilon_{co}$ = strain at peak strength of unconfined concrete.

In a RC column, transverse reinforcements cannot confine the entire core concrete because of the spacing between transverse reinforcements. Therefore, the effective constant confining pressure has to be used instead of the constant confining pressure ($f_l$). The effective constant confining pressure can be calculated by Eq. (4) using the reduction coefficient ($k_e$).

$$f'_l = k_e \cdot f_l \quad (4)$$

### 2.2. Equilibrium in a CFT column

Fig. 5 shows the half section a CFT column when it is under axial load acting on the concrete only. When the stress acting on the outer tube ($f_{ot}$) reaches the yield stress ($f_{oty}$), the constant confining pressure is maximal. From Fig. 5, the constant confining pressure ($f_l$) can be calculated by

$$f_l = \frac{2f_{oty}t_{ot}}{D'} \quad (5)$$

where $t_{ot}$ = thickness of the outer tube, $f_{oty}$ = yield stress of the outer tube, $D'$ = diameter of confined concrete. The concrete in a CFT member is continuously confined along the length of the column by the outer tube. Therefore, a reduction coefficient such as $k_e$ is not required for the CFT column.

### 2.3. Equilibrium in DSCT column

In a DSCT column, the outer tube and the inner tube cooperatively provide the continuous confining pressure on the concrete. Therefore, after one of the tubes fails, the concrete becomes unconfined. Fig. 6 shows the half section of a DSCT column when it is under axial load acting on the concrete only. From Fig. 6a and b, Eqs. (6) and (7) can be derived, respectively. The stress acting on the inner tube ($f_{it}$) is calculated by Eq. (8).

$$f_l(D' - D_i) + 2f_{it}t_{it} = 2f_{ot}t_{ot} \quad (6)$$

$$f_lD_i = 2t_{it}f_{it} \quad (7)$$

$$f_{it} = \frac{f_lD_i}{2t_{it}} \quad (8)$$

where $t_{it}$ = thickness of the inner tube, $D_i$ = outside diameter of the inner tube.

### 2.4. Failure modes

Considering the failures of the inner tube and the outer tube, three failure modes can be defined as Eq. (9). The first failure mode is defined as the inner tube fails by buckling or yielding before the outer tube yields. The reverse is the condition of the second failure mode. In the third failure mode, both tubes fail simultaneously.

$$f_{it} > f_{\lim} = smaller(f_{ity}, f_{bk}) : \text{Failure Mode 1} \quad (9a)$$

$$f_{it} < f_{\lim} = smaller(f_{ity}, f_{bk}) : \text{Failure Mode 2} \quad (9b)$$

$$f_{it} = f_{\lim} = smaller(f_{ity}, f_{bk}) : \text{Failure Mode 3} \quad (9c)$$

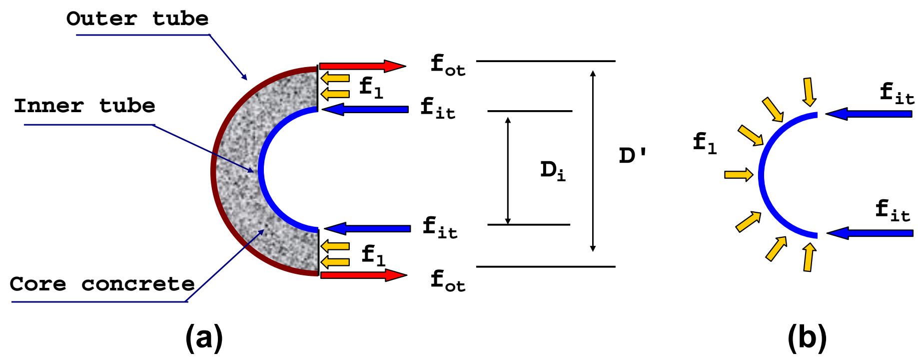


**Fig. 6.** Confining stress on concrete in a DSCT column.

where $f_{ity}$ = yield strength of the inner tube, $f_{bk}$ = buckling strength of the inner tube, and $f_{\lim}$ = smaller value between yield strength and buckling strength of the inner tube.

Optimum performance of a DSCT column is achieved when the inner tube does not fail before the outer tube yields. Yielding failure of the inner tube determines the limit confining pressure on the concrete by the inner tube. Buckling of the inner tube results in a loss of confining pressure.

### 2.5. Yield condition for inner tube

Yielding of the inner tube before the outer tube yields can be guaranteed by controlling the thickness of the inner tube as follows. Eq. (10) is derived from Eqs. (6) and (8). It shows the relation of the stresses acting on the inner and outer tubes. Therefore, Eq. (11) is given and the minimal thickness of the inner tube to prevent its premature yielding failure ($t_y$) is calculated by Eq. (12).

$$f_{it} = \frac{D_i t_{ot}}{D' t_{it}} f_{ot} \tag{10}$$

$$f_{it} = \frac{D_i t_{ot}}{D' t_{it}} f_{oty} < f_{ity} \tag{11}$$

$$t_y = \frac{D_i f_{oty}}{D' f_{ity}} t_{ot} \tag{12}$$

where $f_{ity}$ = yield stress of the inner tube, $t_y$ = required minimal thickness of the inner tube to prevent its premature yielding.

### 2.6. Buckling condition of flat inner tube

The inner tube of a DSCT column is unilaterally restrained by concrete. Because of this unilateral boundary condition, the inner steel tube has a different buckling strength from that of an arch or a ring with bilateral boundary conditions. The buckling strength of unilaterally restrained arches has been studied by many researchers. Kerr and Soifer [17] proposed the buckling strength of a circular arch by linearization of the prebuckling deformation. Haftka et al. [18] suggested the bifurcation buckling strength and snap-through buckling strength of a circular shallow arch using the Koiter's method. When a circular shallow arch is buckled in snap-through behavior, its buckled shape is similar to that of a unilaterally restrained arch. Table 1 presents the buckling load coefficients for circular arch suggested by previous researchers. Sun and Natori [19] proposed the numerical solution of a large deformation problem considering the unilateral boundary condition. Smith and Bradford [20,21] showed that the unilateral buckling strength is larger than the bilateral buckling strength for a rectangular plate subjected to bending, compression and shear. Herzl [22] investigated the contact buckling and postbuckling strength of a thin rectangular plate by experimental method. Papanikolaou and Doudoumis [23] investigated the elastic behavior of rectangular plates with unilateral contact support conditions.

**Table 1**
Circular arch buckling load coefficients.

| Case | Buckling load coefficient | | |
|---|---|---|---|
| | Kerr and Soifer [17] | Haftka et al. [18] | Sun and Natori [19] |
| Bifurcation | 1.91 | 1.86 | 1.90 |
| Snap-through | 2.27 | 2.17 | 2.28 |

In this study, the buckling behavior of the inner steel tube is considered as the snap-through behavior of a circular shallow arch because the inner tube can be buckled only inward. The buckling coefficients proposed by Kerr and Soifer [17] were adopted to estimate the buckling strength of the inner tube. From their study, the buckling strength of a circular shallow arch ($p_0$) can be calculated by Eq. (13). By substituting the snap-through buckling coefficient (2.27) for the normalized nondimensional pressure ($\bar{p}$) in Eq. (14), the buckling strength of the inner tube ($f_{bk}$) can be calculated by Eq. (14).

$$p_0 = \bar{p}\frac{EI}{R^2 t_{it}} \tag{13}$$

$$f_{bk} = 2.27\frac{EI}{R^2 t_{it}} = \frac{2.27}{3}\frac{t_{it}^2 E}{D_i^2} \tag{14}$$

where $E$ = modulus of elasticity, $I$ = moment of inertia, $R$ = radius of the inner tube.

To prevent the premature buckling failure of the inner tube before the outer tube yields, the buckling strength of the inner tube must be larger than the confining pressure acting on concrete when the outer tube yields. With this design concept and Eq. (14), a failure criterion can be defined as Eq. (15). From Eq. (14), the required minimal thickness of the inner tube to prevent its premature buckling failure ($t_{bk}$) can be calculated by Eq. (16). The required minimal thickness of the inner tube to prevent its premature failure ($t_{\lim}$) can be defined as the larger value between $t_y$ and $t_{bk}$ from Eq. (12) and Eq. (16), respectively.

$$f_{bk} = \frac{2.27}{3}\frac{t_{it}^2 E}{D_i^2} > f_l = \frac{2f_{oty}t_{ot}}{D'} \tag{15}$$

$$t_{bk} = \sqrt{\frac{6}{2.27}\frac{D_i^2 f_{oty} t_{ot}}{D'E}} \tag{16}$$

When a DSCT column fails as the failure mode 1, this failure mode can be classified into two failure modes. One is the failure by the yield of the inner tube. The other is the failure by buckling of the inner tube. These failure modes can be determined by the comparison of the yield strength ($f_{ity}$) and the buckling strength ($f_{bk}$) of the inner tube. It is also possible to determine the failure mode with respect to the comparison of the thickness of an inner tube ($t_{it}$) and its required minimal thicknesses for yield ($t_y$) and buckling ($t_{bk}$). Table 2 shows the summary of the failure criteria for a DSCT column.

### 2.7. Buckling condition of corrugated inner tube

When a corrugated tube is used as the inner tube, the failure criteria must be modified because the buckling strength of a corrugated tube is much larger than that of a flat tube. A corrugated plate can be analyzed as a flat plate by replacing the thickness of the plate with an equivalent thickness. For a corrugated plate as shown in Fig. 7, its flexural rigidity of the direction of $y$-axis is given as Eq. (17) when the corrugation is described as a sine function. The moment of inertia ($I$) can be approximately calculated by Eqs. (18) and (19) using height of a wave ($f$) presented by Timoshenko and Krieger [24].

$$D_y = EI \tag{17}$$

$$I = \frac{f^2 t_c}{2}\left[1 - \frac{0.81}{1 + 2.5\left(\frac{f}{2l}\right)^2}\right] \tag{18}$$

$$S = l\left(1 + \frac{\pi^2 f^2}{4l^2}\right) \tag{19}$$

where $l$ = length of one-half a wave, $S$ = arc-length of one-half a wave, and $\nu$ = Poisson's ratio of the corrugated plate, $t_c$ = thickness of the corrugated plate.

If we let $t_{eq}$ be the equivalent thickness of a flat tube which has the equal buckling strength to the corrugated tube, Eq. (20) is derived. Therefore, the failure mode of the DSCT column with a corrugated tube can be defined by calculating its buckling strength by using Eqs. (20) and (14).

$$t_{eq} = \sqrt[3]{6f^2 t_c\left[1 - \frac{0.81}{1 + 2.5\left(\frac{f}{2l}\right)^2}\right]} \tag{20}$$

**Table 2**
Failure criteria of DSCT columns.

| Failure mode | | | Stress criteria | Thickness criteria |
|---|---|---|---|---|
| 1 | A | Yielding of inner tube | $f_{it} > f_{\lim}$ and $f_{bk} > f_{ity}$ | $t_{\lim} > t_{it}$ and $t_y > t_{bk}$ |
| | B | Buckling of inner tube | $f_{it} > f_{\lim}$ and $f_{ity} > f_{bk}$ | $t_{\lim} > t_{it}$ and $t_{bk} > t_y$ |
| | 2 | Yielding of outer tube | $f_{\lim} > f_{it}$ | $t_{it} > t_{\lim}$ |
| | 3 | Simultaneous failure of two tubes | $f_{\lim} = f_{it}$ | $t_{\lim} = t_{it}$ |

Note: $f_{\lim}$ = smaller ($f_{ity}$, $f_{bk}$), $t_{\lim}$ = larger ($t_y$,$t_{bk}$).

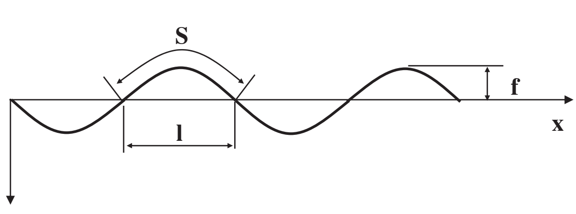


**Fig. 7.** Corrugated plate.

## 3. Summary of application to concrete model in DSCT column

### 3.1. Peak strain and ultimate strain

The concrete in a DSCT column is triaxially confined before the failure of the inner or outer tube. And the confining stress and the maximum strength of the concrete are calculated from Eqs. (5) and (2), respectively. After one of the two tubes fails, the effective confining stress becomes zero. Therefore, an irregular point can be observed on the stress–strain relation path when the inner tube fails. When the outer tube fails, a DSCT column is supposed to be collapsed. The stress–strain relation is given as Eq. (1) and the strain at peak strength of confined concrete ($\varepsilon_{cc}$) is calculated by Eq. (21) suggested by Mander et al. [15].

$$\varepsilon_{cc} = \varepsilon_{co}\left[1 + 5\left(\frac{f'_{cc}}{f'_c} - 1\right)\right] \tag{21}$$

A useful limitation of compressive strain of concrete is when the yielding of outer tube initiates. It may be estimated by equating the strain-energy capacity of the outer tube, which is strained to peak stress ($f_{uh}$). When the outer tube is made of steel, a conservative estimate for ultimate compressive strain ($\varepsilon_{cu}$) is given as Eq. (22) suggested by Mander et al. [15].

$$\varepsilon_{cu} = 0.004 + \frac{1.4\rho_s f_{oty}\varepsilon_{su}}{f'_c} \tag{22}$$

where $\varepsilon_{su}$ = strain of steel at maximum tensile stress, $\rho_s$ = volumetric ratio of confining steel to the concrete.

### 3.2. Axial strength of DSCT column

When the DSCT column member is axially compressed, the three components, inner tube, outer tube, and the concrete, are supposed to be subjected to the same axial strain. The axial load sustained at this strain is the sum of the forces acting on the three components.

$$N = A_c f_c + A_{it} f_{itz} + A_{ot} f_{otz} \tag{23}$$

where $A_c$, $A_{it}$ and $A_{ot}$ = cross-sectional areas of the concrete, inner tube and outer tube, respectively. $f_{itz}$ and $f_{otz}$ = axial stresses of the inner tube and the outer tube, respectively.

## 4. Numerical evaluation and parametric study

A FORTRAN computer program was developed using the new concrete model for a DSCT column. Fig. 8 shows the analysis procedure to determine the stress–strain relationship of the concrete in a DSCT column member. The developed program was verified by the experimental results from other researchers. And using the developed program, some example models were analyzed for DSCT column members having a flat inner tube (DSCT-F) and a corrugated inner tube (DSCT-C).

### 4.1. Verification with experimental results

To verify the stress–strain model for the concrete of DSCT columns, several CFT columns ($D_i = 0$) and a DSCT column were analyzed and compared with the experimental results by Im et al. [25] and Wei et al. [3], respectively. A CFT column can be regarded as the DSCT column whose hollow ratio is zero. Therefore, the thickness of the outer tube is the main parameter for the CFT column. The confined concrete of the example model has the diameter of 100 mm. Its height is 200 mm. The strength of the unconfined concrete is 27.65 MPa. The yield strength of the outer tube and its maximal strain are 235.44 MPa and 0.2, respectively. The outer tube has

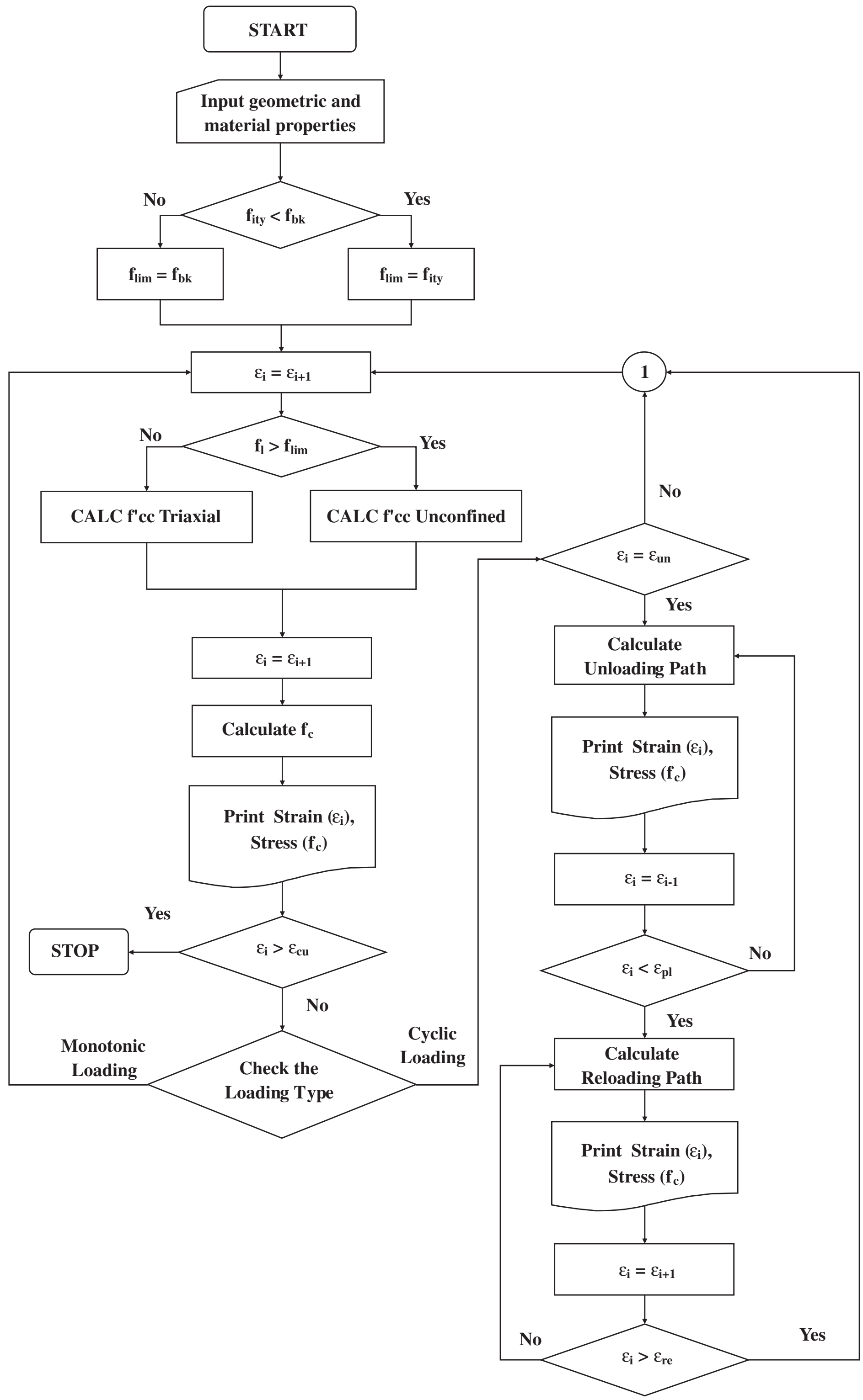


**Fig. 8.** Calculation procedure for proposed stress–strain model of concrete in DSCT column.

the modulus of elasticity of 206 GPa. Fig. 9 shows stress–strain relations of concrete in a CFT column as the thickness of the outer tube varies. As the thickness of the outer tube increases, the concrete has larger strength and ductility. Fig. 10 shows the unloading path and reloading path of the concrete in a CFT column when the thickness of the outer tube is 0.8 mm. Figs. 11 and 12 show the verifications with the experimental results by Im et al. [25]. The outer tube of the model shown in Fig. 11 has the thickness of 1.2 mm. The other geometric and material properties are equal to those of the models in Fig. 9. The model shown in Fig. 12 has the outer tube with the thickness of 1.0 mm and its unconfined concrete strength is 23.89 MPa. The other geometric and material properties are equal to those of the models in Fig. 9.

Fig. 13 shows the verification of the developed model with the experimental result from Wei et al. [3]. The sum of the strengths of three components (Eq. (23)) agrees with the test result because the

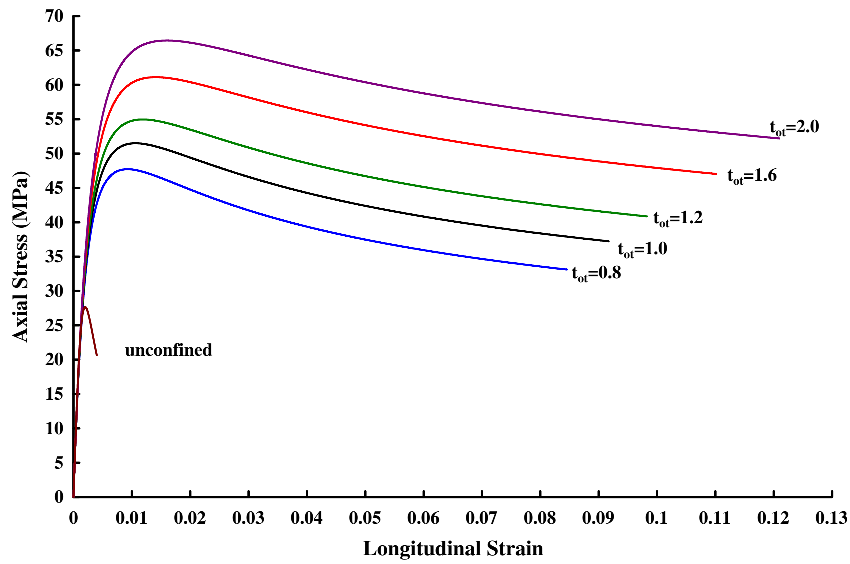


**Fig. 9.** Stress–strain relations of concrete in CFT column members.

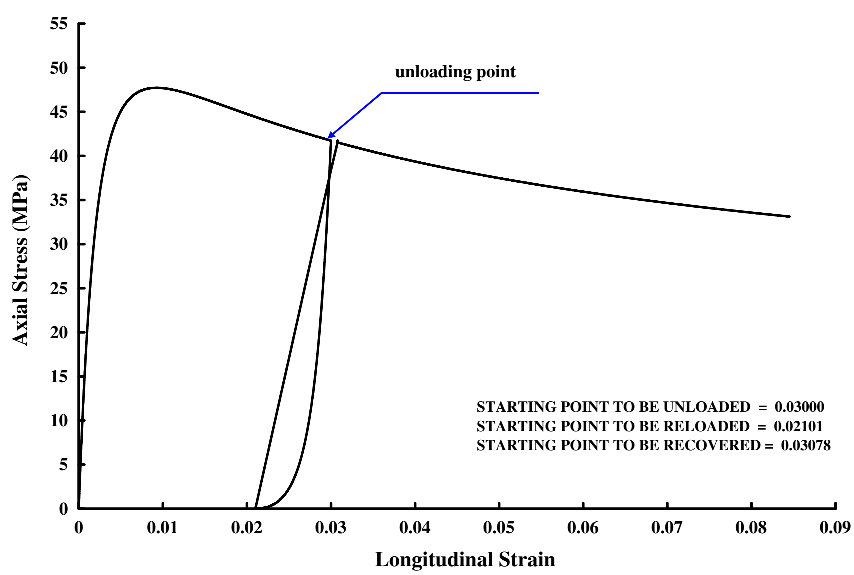


**Fig. 10.** Stress–strain relation of concrete in CFT column member under cyclic load ($t_{ot}$ = 0.8).

increased strength of the confined concrete was considered. The unconfined strength of the concrete was 60 MPa. The geometric and material properties of the test specimen are summarized in Table 3. $E_{it}$ and $E_{ot}$ are moduli of elasticity of the inner tube and outer tube, respectively.

### 4.2. DSCT column with a flat inner tube

Parametric studies for the concrete in a DSCT column with a flat inner tube were performed. The analyzed model had the outer tube with the diameter of 2000 mm ($D'$ = 2000 mm) and the thickness of 10 mm. Its modulus of elasticity, yield strength, and ultimate strain were 206 GPa, 196.2 MPa, and 0.2, respectively. The inner tube had the yield strength of 294.3 MPa and its modulus of elasticity was 206 GPa. The hollow ratio ($D_i/D'$), the thickness of the inner tube, and the unconfined strength of concrete ($f_c'$) were selected as the main parameters in the analysis.

Figs. 14 and 15 show the stress–strain relations of the concrete in the DSCT columns when their hollow ratios are 0.7 and 0.8 respectively. In these analyses, the unconfined strength of the concrete was 25 MPa and the thickness of the inner tube was varied. For the columns of Fig. 14, the required minimal thicknesses of the inner tube are calculated as $t_y$ = 4.67 mm and $t_{bk}$ = 4.97 mm. Therefore, in the plots where the thickness of the inner tube is 1 mm or 3 mm, the inner tube buckles. And the stress–strain plot of the concrete drops sharply indicating premature failure due to the loss of confining pressure. In the plots where the thickness of the inner tube is greater than $t_{\mathrm{lim}}$ (=4.97 mm), the stress–strain plot of the concrete is complete and the peak concrete stress is limited by the yield strength of the outer tube. For the columns of Fig. 15, the required thicknesses of the inner tube are calculated as $t_y$ = 5.34 mm and $t_{bk}$ = 5.67 mm. Therefore, in the plots where the thickness of the inner tube is 1 mm, 3 mm, or 5 mm, the inner tube buckles and the concrete stress–strain plot drops sharply indicating premature failure due to the loss of confinement. For plots where the thickness of the inner tube is greater than $t_{\mathrm{lim}}$ (=5.67 mm), the concrete stress–strain plot is complete and the peak concrete stress is limited by the yield strength of the outer

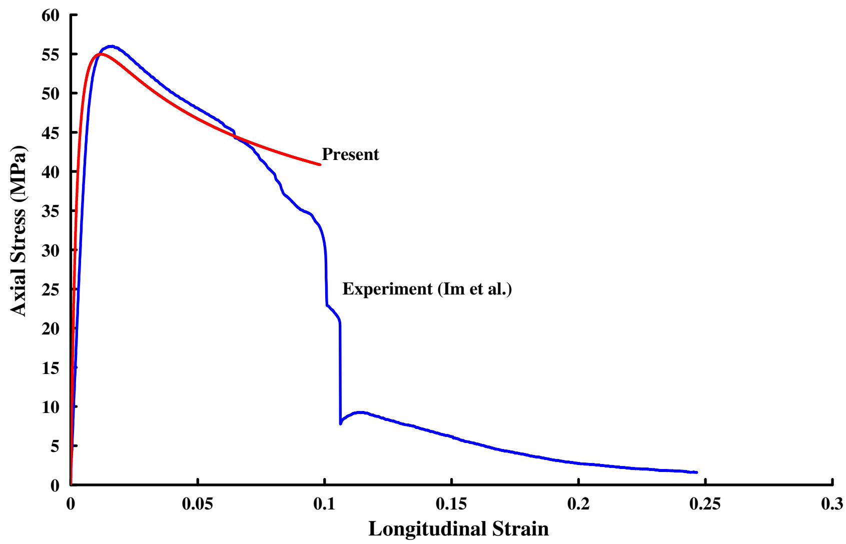


**Fig. 11.** Model verification ($f'_c$ = 27.65 MPa, $t_{ot}$ = 1.2 mm).

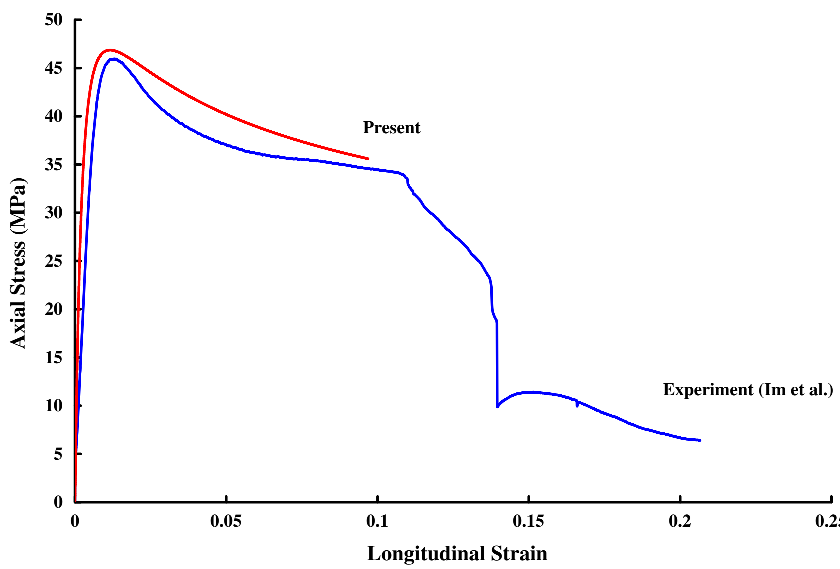


**Fig. 12.** Model verification ($f'_c$ = 23.89 MPa, $t_{ot}$ = 1.0 mm).

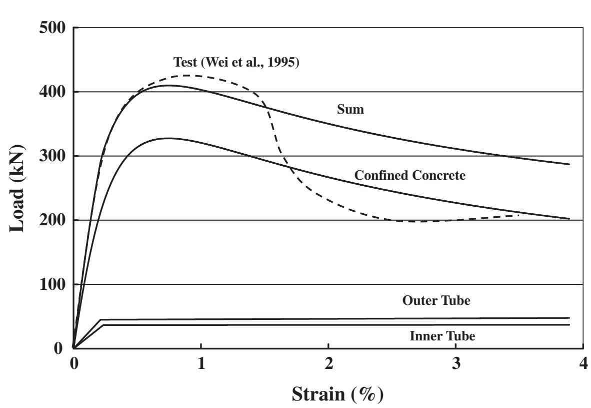


**Fig. 13.** Comparison between analysis and test result for the strength of DSCT column member.

**Table 3**
Geometric and material properties of the test specimen [3,4].

| Geometric property | | Material property | |
|---|---|---|---|
| $D'$ (mm) | 99.9 | $f_{ity}$ (MPa) | 512 |
| $D_i$ (mm) | 74.0 | $f_{oty}$ (MPa) | 409 |
| $t_{it}$ (mm) | 0.62 | $E_{it}$ (GPa) | 219 |
| $t_{ot}$ (mm) | 0.70 | $E_{ot}$ (GPa) | 193 |

tube. In Figs. 14 and 15, when the inner tube does not fail before the outer tube yields, the stress–strain relation plots are overlapped.

Fig. 16 shows stress–strain relations of the concrete in the DSCT columns with different hollow ratios. Their inner tubes have a thickness of 3 mm and the other geometric and material properties are same as for the prior analysis models except the hollow ratio.

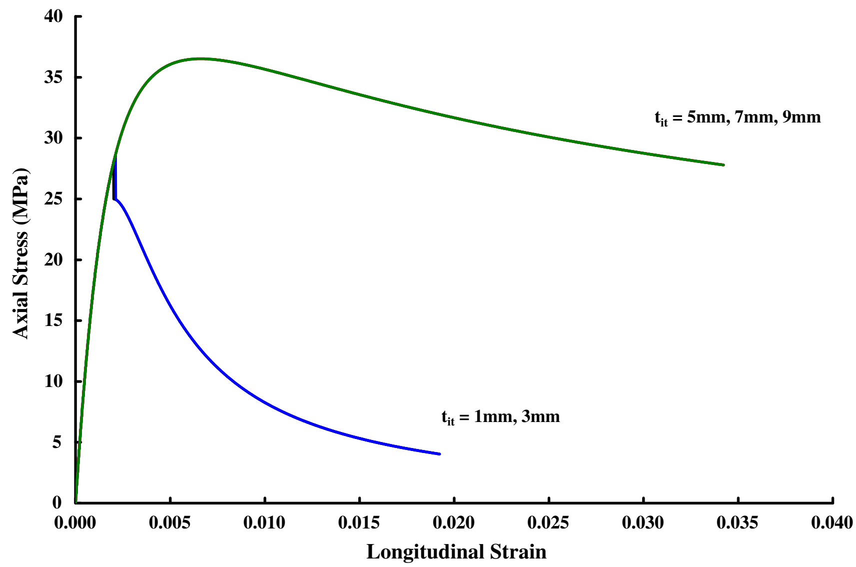


**Fig. 14.** Stress–strain relation of concrete in DSCT column member ($D' = 2000$ mm, $D_i = 1400$ mm).

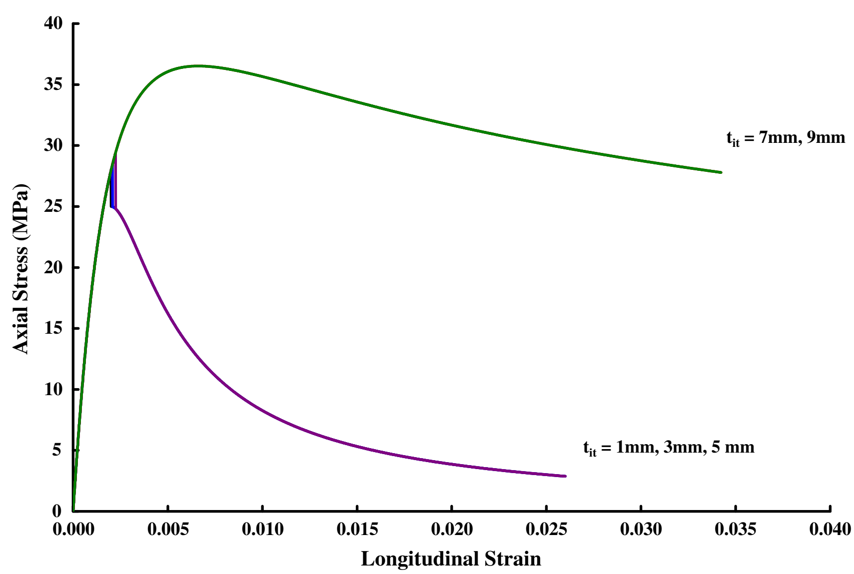


**Fig. 15.** Stress–strain relation of concrete in DSCT column member ($D' = 2000$ mm, $D_i = 1600$ mm).

The hollow ratio was varied in the range of 0.1 to 0.8. Because the hollow ratio is different for every column model, $t_{\lim}$ is also different as shown in Table. 4. When the hollow ratio is smaller than 0.5, the concrete in the DSCT column is completely confined until the outer tube yields. But the inner tube is buckled in the reverse condition. Fig. 17 shows stress–strain relations of the concrete in the DSCT columns with various unconfined concrete strengths. The hollow section of the DSCT column has the diameter of 1400 mm. The inner tube has the thickness of 5 mm. The strengths of the unconfined concrete are 20, 22, 24, 26 and 28 MPa. They show slightly lower ductility as their strength increases. Fig. 18 shows their confined strengths, increased amounts of the strength, and increased ratios of the strength. It shows that their increased strengths are almost constant under the equal conditions although their unconfined concrete strengths are different. This result means that the confining effect is more significant for the low-strength concrete.

### *4.3. DSCT column with a corrugated inner tube*

A parametric study for the concrete in a DSCT column with a corrugated inner tube (DSCT-C column) was performed. The outer tube had the diameter of 2000 mm ($D' = 2000$ mm) and the thickness of 10 mm. Its modulus of elasticity, yield strength, and ultimate strain were 206 GPa, 196.2 MPa, and 0.2, respectively. The inner tube had the yield strength of 294.3 MPa. Its modulus of elasticity was 206 GPa. The unconfined strength of the concrete ($f_c'$) was 25 MPa. The corrugation of the inner tube had the wave height ($f$) of 20 mm and the length of one-half a sine wave ($l$) of 50 mm.

Fig. 19 shows the stress–strain relations of the concrete in the DSCT-C columns with the hollow ratio of 0.75. The required minimal thicknesses of the inner tube are calculated as $t_y = 5$ mm and $t_{bk} = 0.714$ mm. Therefore, the corrugated inner tube which has the thickness of 1 mm or 3 mm yields. When the thickness of the inner tube is larger than 5 mm, the concrete exerted its confined

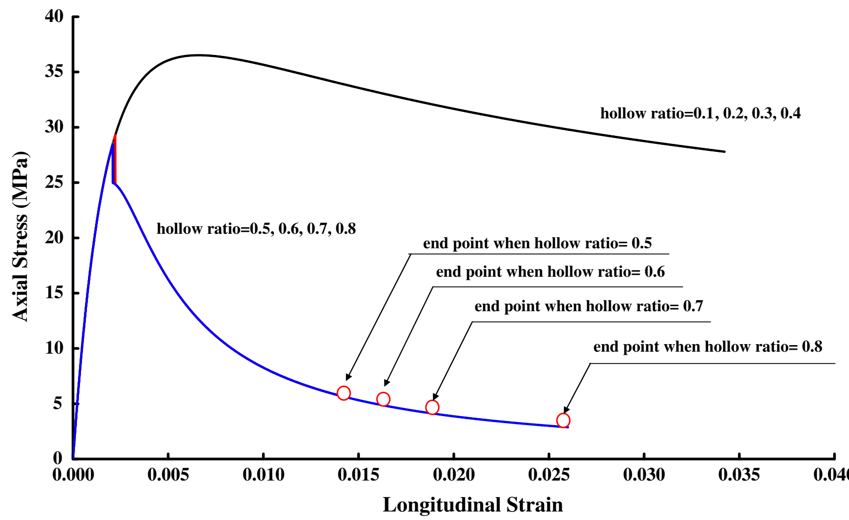


**Fig. 16.** Effects of hollow ratio on stress–strain relation of concrete ($t_{it}$ = 3 mm, $t_{ot}$ = 10 mm).

**Table 4**
Required thickness of inner tube and failure mode.

| Required thickness | Hollow ratio | | | | | | | |
|---|---|---|---|---|---|---|---|---|
| | 0.1 | 0.2 | 0.3 | 0.4 | 0.5 | 0.6 | 0.7 | 0.8 |
| $t_y$ (mm) | 0.067 | 0.133 | 0.200 | 0.267 | 0.333 | 0.400 | 0.467 | 0.533 |
| $t_{bk}$ (mm) | 0.071 | 0.142 | 0.213 | 0.284 | 0.355 | 0.426 | 0.497 | 0.568 |
| $t_{\lim}$ (mm) | 0.071 | 0.142 | 0.213 | 0.284 | 0.355 | 0.426 | 0.497 | 0.568 |
| Failure mode | 2 | 2 | 2 | 2 | 1B | 1B | 1B | 1B |

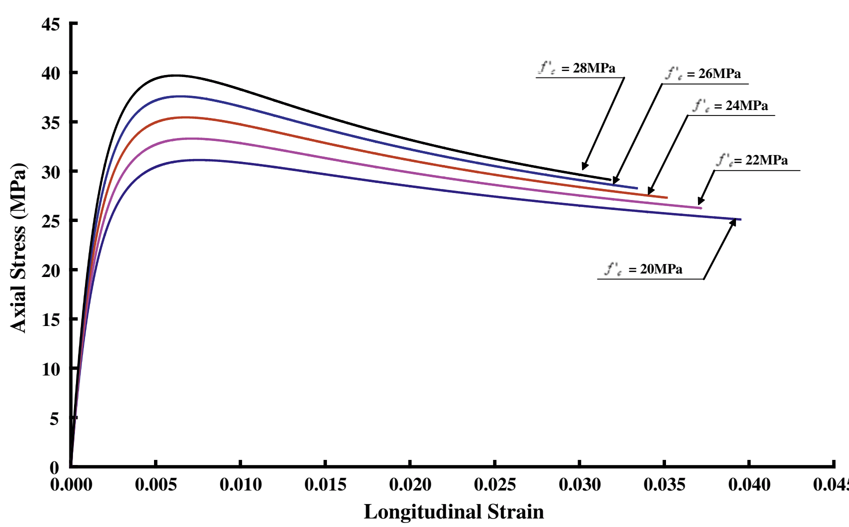


**Fig. 17.** Comparison of stress–strain relations of confined concrete with different unconfined strength.

strength completely until the outer tube yields. When the thickness of the inner tube is 5 mm, the inner tube and the outer tube fail simultaneously.

Fig. 20 shows loading, unloading, and reloading paths of the concrete in the DSCT-C column with the hollow ratio of 0.8. The thickness of the inner tube is 3 mm and the other properties are same with the previous models of Fig. 19. Because the corrugated inner tube yields prematurely, the stress–strain path shifts at the point where the inner tube fails (irregular point). To show the magnified unloading and reloading paths, the graph was omitted after the strain of 0.004.

## 5. Summary and conclusions

A nonlinear concrete model for DSCT columns was developed that accounts for the effect of confinement on the strength of the concrete. The developed concrete model was based on the uniaxial

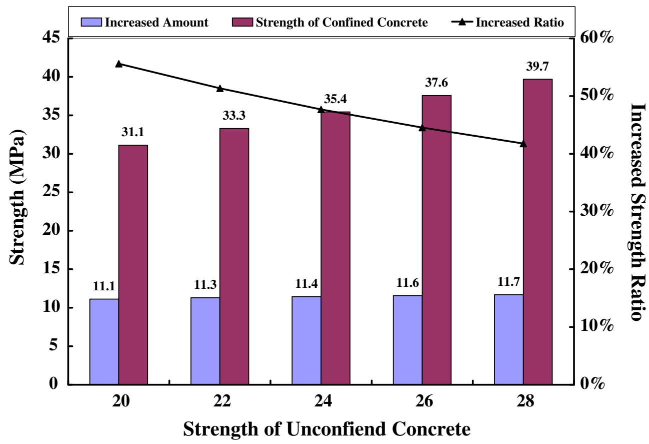


**Fig. 18.** Comparison of stress–strain relations of confined concrete with different unconfined strength.

stress–strain model proposed by Mander et al. [15]. And it was extended for the DSCT column using the definitions of confining pressure by several failure modes. When the inner tube does not fail before the yield failure of the outer tube, the concrete in the DSCT column is confined triaxially until the column fails. The confined concrete shows much higher strength than unconfined concrete. This explains why the DSCT column shows higher strength than the sum of the strengths of inner tube, outer tube, and concrete alone. When the inner tube fails by buckling or yielding before the outer tube fails, the concrete in the DSCT column is in the unconfined state. It results in a premature failure of the column. The strength and ductility of the concrete in the DSCT column can be controlled by the thickness of the inner tube as well as the thickness of the outer tube. The thickness of the inner tube should satisfy the minimal requirement for the safety of the column. To reduce material and to maximize buckling strength of the inner tube, a corrugated inner tube can be used.


## Acknowledgement

This work was supported by the Korea Science and Engineering Foundation (KOSEF) through the National Research Lab. Program funded by the Ministry of Science and Technology (No. R0A-2005-000-10119-0).


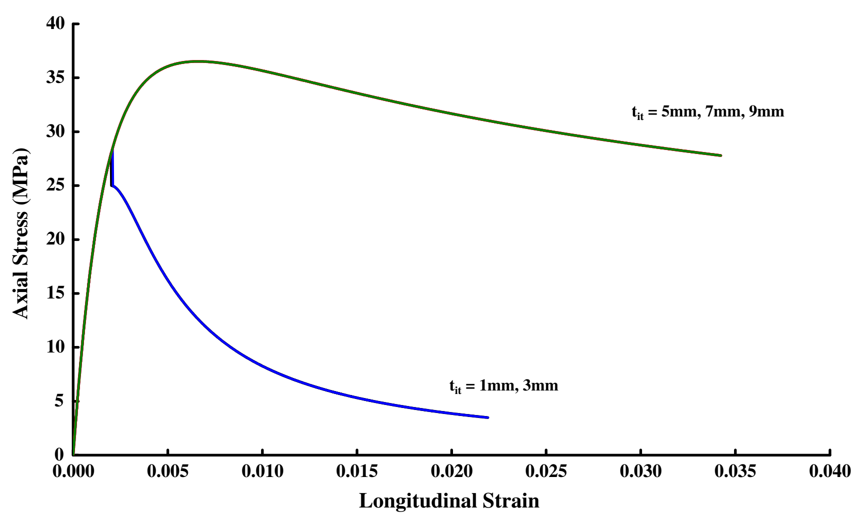


**Fig. 19.** Stress–strain relation of concrete in DSCT-C column member ($D' = 2000$ mm, $D_i = 1500$ mm).

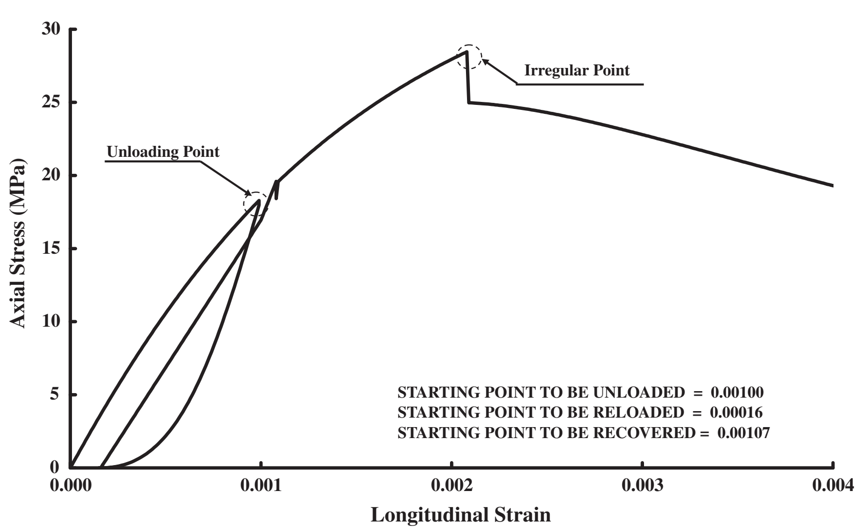


**Fig. 20.** Unloading and reloading path of concrete ($D' = 2000$ mm, $D_i = 1600$ mm).

## References


[1] Han TH, Lim NH, Han SY, Park JS, Kang YJ. Nonlinear concrete model for an internally confined hollow reinforced concrete column. Mag Concr Res 2008;60(6):429–40.

[2] Shakir-Khalil H, Illouli S. Composite columns of concentric steel tubes. In: Proceeding of conference on the design and construction of non conventional structures; 1987. p. 73–82.

[3] Wei S, Mau ST, Vipulanandan C, Mantrala SK. Performance of new sandwich tube under axial loading: experiment. J Struct Eng 1995;121(12):1806–14.

[4] Wei S, Mau ST, Vipulanandan C, Mantrala SK. Performance of new sandwich tube under axial loading: analysis. J Struct Eng 1995;121(12):1815–21.

[5] Zhao X-L, Grzebieta R. Strength and ductility of concrete filled double skin (SHS inner and SHS outer) tubes. Thin-Walled Struct 2002;40:199–213.

[6] Tao Z, Han L-H, Zhao X-L. Behavior of concrete-filled double skin (CHS inner and CHS outer) steel tubular stub columns and beam columns. J Constr Steel Res 2004;60:1129–58.

[7] Han TH, Han KH, Han SY, Kim SN, Kang JO, Kang YJ. The behavior of an internally confined hollow concrete filled steel tube column. In: Proceeding of the 8th Korea–Japan joint seminar; 2005. p. 433–41.

[8] Teng JG, Yu T, Wong YL, Dong SL. Hybrid FRP-concrete-steel tubular columns: concept and behavior. Constr Build Mater 2006;21:846–54.

[9] Yu T, Wong YL, Teng JG, Dong SL, Lam ESS. Flexural behavior of hybrid FRP-concrete–steel double-skin tubular members. J Compos Constr, ASCE 2006;10(5):443–52.

[10] Roy HEH, Sozen MA. Ductility of concrete. In: Proceedings of the international symposium on the flexural mechanics of reinforced concrete, ASCE-ACI; 1964. p. 213–24.

[11] Popovics S. A numerical approach to the complete stress–strain curves of concrete. Cem Concr Res 1973;3(5):583–99.

[12] Kent DC, Park R. Flexural members with confined concrete. ASCE 1971;97(ST.7):1969–90.

[13] Leslie PD. Ductility of reinforced concrete bridge piers. M.E. Report, University of Canterbury, New Zealand; 1974.

[14] Desayi P, Iyengar KTSR, Reddy TS. Equations of stress–strain curve of concrete confined in circular steel spiral. Mater Constr 1978(September/October):339–45.

[15] Mander JB, Priestley MJN, Park R. Seismic design of bridge piers. Research report no. 84-2, Univ. of Canterbury, New Zealand; 1984.

[16] Candappa DC, Sanjayan JG, Setunge S. Complete triaxial stress–strain curves of high-strength concrete. J Mater Civil Eng 2001(May/June):209–15.

[17] Kerr AD, Soifer MT. The linearization of the prebuckling state and its effects on the determined instability load. J Appl Mech 1969;36:775–85.

[18] Haftka RT, Mallet RH, Nachbar W. Adaptation of Koiter's method to finite element analysis of snap-through buckling behavior. Int J Solid Struct 1971;7:1427–45.

[19] Sun SM, Natori MC. Numerical solution of large deformation problems involving stability and unilateral constraints. Comput Struct 1996;58(6):1245–60.

[20] Smith ST, Bradford MA, Oehlers DJ. Elastic buckling of unilaterally constrained rectangular plates in pure shear. Eng Struct 1999;21:443–53.

[21] Bradford MA, Smith ST, Oehlers DJ. Semi-compact steel plates with unilateral restraint subjected to bending, compression, and shear. J Constr Steel Res 2000;56:47–67.

[22] Herzl C. Contact buckling and postbuckling of thin rectangular plates. J Mech Phys Solids 2001;49:209–30.

[23] Papanikolaou VK, Doudoumis IN. Elastic analysis and application tables of rectangular plates with unilateral contact support conditions. Comput Struct 2001;79:2559–78.

[24] Timoshenko SP, Woinowsky-Krieger S. Theory of plates and shells. Singapore: McGraw-Hill, Inc.; 1959.

[25] Im SB, Han TH, Han SY, Kang YJ. Stress–strain relations of concrete according to the confining conditions. J Korean Soc Civil Eng 2006;26(4A):743–52.